L-Dopa activates histaminergic neurons

Yevgenij Yanovsky[1], Sha Li[1,2], Boris P. Klyuch[1], Qiaoling Yao[2], Patrizio Blandina[3], M. Beatrice Passani[3], Jian-Sheng Lin[2], Helmut L. Haas[1] and Olga A. Sergeeva[1]

[1]*Department of Neurophysiology, Heinrich-Heine-University, D-40001, Dusseldorf, Germany*
[2]*INSERM-U628, Physiologie intégrée du système d'éveil, 69373 Lyon Cedex 08, France*
[3]*Dipartimento di Farmacologia Preclinica e Clinica Viale Pieraccini 6, 50139 Firenze, Italy*

Non-technical summary L-Dopa is an effective medication for Parkinson's disease (PD), but loses efficiency with time. This can be delayed by treatment with histamine antagonists. We show histaminergic neurons in the hypothalamus controlling wakefulness are excited by L-Dopa, which they can take up and transform to dopamine. They innervate the whole brain, in particular the striatum which is deficient of dopamine in PD. We revealed mechanisms of excitation of histaminergic neurons by L-Dopa and dopamine opening new avenues for the treatment of PD and sleep disorders.

Abstract L-Dopa is the most effective treatment of early and advanced stages of Parkinson's disease (PD), but its chronic use leads to loss of efficiency and dyskinesia. This is delayed by lower dosage at early stages, made possible by additional treatment with histamine antagonists. We present here evidence that histaminergic tuberomamillary nucleus (TMN) neurons, involved in the control of wakefulness, are excited under L-Dopa (EC_{50} 15 μM), express Dopa decarboxylase and show dopamine immunoreactivity. Dopaergic excitation was investigated with patch-clamp recordings from brain slices combined with single-cell RT-PCR analysis of dopamine receptor expression. In addition to the excitatory dopamine 1 (D1)-like receptors, TMN neurons express D2-like receptors, which are coupled through phospholipase C (PLC) to transient receptor potential canonical (TRPC) channels and the Na^+/Ca^{2+} exchanger. D2 receptor activation enhances firing frequency, histamine release in freely moving rats (microdialysis) and wakefulness (EEG recordings). In histamine deficient mice the wake-promoting action of the D2 receptor agonist quinpirole (1 mg kg^{-1}, I.P.) is missing. Thus the histamine neurons can, subsequent to L-Dopa uptake, co-release dopamine and histamine from their widely projecting axons. Taking into consideration the high density of histaminergic fibres and the histamine H3 receptor heteromerization either with D1 or with D2 receptors in the striatum, this study predicts new avenues for PD therapy.

(Received 27 November 2010; accepted after revision 11 January 2011; first published online 17 January 2011)
Corresponding author O. A. Sergeeva: Heinrich-Heine-Universität, Department of Neurophysiology, D-40001 Düsseldorf, Germany. Email: olga.sergeeva@uni-duesseldorf.de

Abbreviations DA, dopamine; DAT, dopamine transporter; DDC, Dopa decarboxylase; EEG, electroencephalogram; D2R, dopamine receptor 2; EMG, electromyogram; H3R, histamine receptor 3; HDC, histidine decarboxylase; PS, paradoxical sleep; scRT-PCR, single-cell RT-PCR; SWS, slow wave sleep; TH, tyrosine hydroxylase; TMN, tuberomamillary nucleus; VMAT2, vesicular monoamine transporter type 2.

Y. Yanovsky, S. Li and B. P. Klyuch contributed equally to the study.

DOI: 10.1113/jphysiol.2010.203257

The Journal of Physiology

Introduction

Parkinson's disease (PD) is characterized by slowness of movement (bradykinesia), increased muscle tone (rigidity) and tremor. Progressive loss of nigral neurons with Lewy bodies is considered a hallmark of PD. Other dopaminergic cells remain intact, including hypothalamic neurons (Purba *et al.* 1994). PD symptoms appear when the concentration of dopamine drops to 20–30% (reviewed in Mercuri & Bernardi (2005)). Sleep dysfunction, a typical non-motor symptom of PD, may result from degeneration of arousal systems including the locus coeruleus (noradrenalin), the pedunculo-pontine nucleus and the basal forebrain (acetylcholine), the median raphe (serotonin) and the lateral hypothalamus (orexin) (Saper *et al.* 1991; Fronczek *et al.* 2007; Arnulf & Leu-Semenescu, 2009). The histaminergic system remains relatively intact in PD (Anichtchik *et al.* 2000) and can modulate, through H3 heteroreceptors, dopaminergic, serotonergic, noradrenergic, cholinergic, glutamatergic and other neurons involved in the control of cortical arousal (Haas *et al.* 2008; Lin *et al.* 2011). Histamine H3 receptor (H3R) antagonism increases vigilance, attention and cognition in PD patients (Arnulf & Leu-Semenescu, 2009).

Von Economo (1926) demonstrated a critical role of the posterior hypothalamus in the control of vigilance showing lesions in this brain area in patients with encephalitis lethargica. It is very likely that the histaminergic and the orexinergic neurons were damaged in these patients. Both neuronal groups are located in the posterior hypothalamus and send diffuse projections to most parts of the brain (Jones, 2005; Saper, 2006; Haas *et al.* 2008). They provide a complementary and synergistic control of waking: the former orchestrates the motor, behavioural and emotional components, the latter cognitive aspects of arousal (Anaclet *et al.* 2009).

Surprisingly, neither orexin nor histamine deficiency results in a major impairment of wake amount, whereas dopamine transporter (DAT) knockout mice depleted of dopamine (Sotnikova *et al.* 2006) do not sleep and do not move (Dzirasa *et al.* 2006). Dopamine acts through five subtypes of G protein-coupled receptors. According to their pharmacological, biochemical and physiological properties, they are divided into two subfamilies (Dziedzicka-Wasylewska, 2004): the D1-like receptor subfamily, D1 and D5 receptors, which are positively coupled to adenylyl cyclase and the D2-like receptor subfamily, D2, D3 and D4 receptors, which are either not or negatively coupled to adenylyl cyclase (Stoof & Kebabian, 1984; Onali *et al.* 1985; Memo *et al.* 1986). D1Rs mediate behavioural arousal, while D2R activation induces somnolence at low but waking at larger doses (Monti & Monti, 2007).

Quinpirole, a D2-like receptor agonist, restores REM sleep in mice totally depleted of dopamie (Dzirasa *et al.* 2006). Similarly, PD patients treated with dopamine receptor agonists experience two- to threefold more sleep attacks than those on laevodopa (L-Dopa) therapy (Arnulf & Leu-Semenescu, 2009). The superior effect of L-Dopa medication in PD is still poorly understood (Mercuri & Bernardi, 2005). Disadvantages of the L-Dopa treatment, such as loss of effectivity during disease progression, dyskinesia and psychotic events, could perhaps be overcome if we better understand the interplay between the neuronal circuitries affected by L-Dopa. As an anti-H3R medication is wake-promoting in PD patients (Arnulf & Leu-Semenescu, 2009; Arnulf, 2009), information is warranted on the histaminergic system's response to 'classical' (co)medications such as dopaminergic agonists or L-Dopa.

Methods

All methods required to obtain tissue for *in vitro* experiments and the *in vivo* recordings were performed in accordance with the ethical standards of *The Journal of Physiology* as set out by Drummond (2009).

Animals and slice recordings

Animal experiments were conducted according to German law (Tierschutzgesetz BGBl. I,S. 1206, revision 2006), EEC directives 86/609/EEC and local guidelines (LANUV FB Tierschutz, Bezirksregierung Duesseldorf). All efforts were made to minimize the number of animals and their suffering. Rodents were killed by neck dislocation and decapitation by appropriately trained staff. Coronal brain slices from the posterior hypothalamus with a thickness of about 450 μm (for conventional slice recording) or 300 μm (for recording under DIC microscopy) containing the tuberomamillary nucleus (TMN) were prepared from 25- to 28-day-old male Wistar rats and 5- to 10-week-old histidine decarboxylase knockout mice or their wild-type littermates (for details see Parmentier *et al.* 2009)).

Extracellular recordings were obtained using glass microelectrodes filled with artificial cerebrospinal fluid (ACSF) (resistance 4–8 MΩ). According to Ericson *et al.* (1987) the TMN is subdivided into three subgroups: a diffuse part (neurons are scattered within the lateral hypothalamic area) and two compact (nucleus-like) parts: the ventral TMN (neurons situated at the ventral surface of the brain) and the medial TMN (dense neuronal groups on each side of the mamillary recess of the third ventricle). Neurons were recorded in the ventral, most dense part of TMN (TMNv). Neurons were assigned as TMN neurons and used for the analysis if they had regular firing in the range of 1–6 Hz (most typically

2–4 Hz), broad action potentials (2–4 ms) and were inhibited by the H3-receptor agonist α-methyl-histamine (Sergeeva *et al.* 2006). Signals were recorded using an Axoclamp 2B amplifier (Axon Instruments, USA), filtered between 0.5–10 kHz, sampled at 20 kHz and analysed with pCLAMP8 software (Axon Instruments). The frequency of extracellular action potentials was determined online in bins of 15 s duration.

For the patch-clamp recordings, TMNv neurons were visualized and approached under infrared light and differential interference (IR-DIC) optics by the placement of an adequate filter (780 nm; R69, Schott, Germany) in the light path. A fixed stage upright compound microscope, Zeiss Axioscope2 FS (Zeiss, Oberkochen, Germany) with corresponding DIC optics and NA condenser was used. The image was detected with an infrared-sensitive video camera (Newvicon C2400; Hamamatsu, Hamamatsu City, Japan). The TMNv neurons exhibited a regular spontaneous discharge at a typical rate of 2–6 Hz and no burst firing. In whole-cell configuration, histaminergic neurons were identified by the presence of the inwardly rectifying current activated by hyperpolarization (I_h) and the transient outward current (I_A; Haas & Reiner, 1988). A square pulse (50 mV amplitude and 1 s duration) was applied to evoke I_h. Only neurons fulfilling these criteria for identification were considered for further analysis. The patch pipettes (resistance 4.5–5 MΩ) were made from 1.5 mm (OD) borosilicate glass (Science Products GmbH, Hofheim, Germany) using a horizontal micro-electrode puller (P-87, Sutter Instrument Co., Novato, CA, USA). For whole-cell recordings, the pipettes were filled with (in mM): KCl 130, NaCl 10, $MgCl_2$ 2, $CaCl_2$ 0.25, glucose 5, Hepes 5, EGTA 10, Mg-ATP 5, Mg-GTP 0.3, pH 7.3 adjusted with 1 M KOH. Biocytin (1%, Sigma, Deisenhofen) was added to the electrode solution in some experiments. To examine the effect of low extracellular sodium on the amplitude and *I–V* curve of the quinpirole-induced inward current, ACSF containing low sodium was prepared by replacing 124 mM of NaCl with an equimolar concentration of *N*-methyl-D-glucamine (NMDG) (pH 7.3 with 1 M HCl). Patch-clamp recordings were performed using an EPC7 patch-clamp amplifier (Heka Electronik, Lambrecht/Pfalz, Germany). After identification of neurons properties, the holding potential (V_h) was set to −70 mV. Steady-state current–voltage (*I–V*) plots were obtained by ramping the membrane potential from +45 to −130 mV at a rate 0.01 mV ms^{-1} before and during D2 agonist application. The net current–voltage plot of the quinpirole-induced inward current was obtained by digital subtraction of the control *I–V* curve from that obtained in the presence of quinpirole. The values of membrane potential were corrected for the liquid junction between the pipette and the bath solutions (2.4 mV, calculated using the build-in software in pCLAMP9). Voltage signals and synaptic currents were filtered at 3 kHz with a four-pole Bessel filter, sampled at 10 kHz using pCLAMP9 software, and stored on a PC for off-line analysis. Cells were discarded if their capacitance transients changed during recordings by more than 10%.

Spontaneous gabazine-sensitive inhibitory post-synaptic currents were recorded in the presence of tetrodotoxin (TTX; 1 μM), D(−)-2-amino-5-phosphonopentanoic acid (D-AP5; 50 μM) and 6,7-dinitro-quinoxaline-2,3-dione (DNQX; 20 μM) and represented therefore spike-independent GABAergic miniature inhibitory postsynaptic currents (mIPSCs). The experimental protocol included at least 20 min control, 12 min application of quinpirole and at least 20 min washout periods. Holding potential was –70 mV. Miniature IPSCs were analysed with MiniAnalysis 4.2 (Synaptosoft, Decatur, GA, USA): Peak amplitude, the 10–90% rise time, decay time to 0.1% of peak and frequency of sIPSCs were calculated. All events were visually inspected before analysis in order to exclude obvious artefacts. Cumulative inter-event intervals, kinetics (τ_{dec}) and amplitudes were compared between control (before quinpirole application) *versus* a period of recording with quinpirole and washing out using the Kolmogorov–Smirnov two-sample test in every cell. Statistical analysis was made using the Prism5 software (GraphPad Software Inc., La Jolla, CA, USA). Student's paired and unpaired, two-tailed *t* test and Wilcoxon's non-parametric test were used to determine changes and differences were considered statistically significant if $P < 0.05$. Data are presented as means ± standard error of mean (SEM).

Microdialysis in freely moving rats

All experiments followed EEC (86/609/EEC) directives. Male Sprague–Dawley rats (250–280 g) were anaesthetized with chloral hydrate (400 mg kg^{-1} I.P.) and implanted with a guide cannula according to the following coordinates from bregma: TMN, AP = −4.3, L = −1.1, DV = +7.2. The microdialysis experiments were performed 48 h after surgery. The stylet was removed from the guide cannulae, and microdialysis probes (molecular mass cut-off = 6000 Da, Metalant AB, Stockholm, Sweden) were inserted; the dialysing membrane protruded 2 mm from the tip of the cannula. Histamine release stabilized 2 h after insertion of the microdialysis probes, and fractions were collected at 15 min intervals. The placement of microdialysis membranes was verified *post mortem*. HA contents in the dialysates were determined by HPLC-fluorimetry as previously described (Cenni *et al.* 2006).

Immunohistochemistry

To reveal histamine and tyrosin hydroxylase immunoreactivities, hypothalamic slices containing the TMN region were fixed overnight in 4% 1-ethyl-3(3-dimethylaminopropyl)-carbodiimide (EDAC) in 0.1 M sodium phosphate buffer (pH 7.4) and post-fixed for 30 min in 4% paraformaldehyde in 0.1 M phosphate buffer (PB), pH 7.4 and cryoprotected in PB with 20% sucrose. Slices were cryosectioned at 25 μm thickness. Sections were mounted on gelatin-coated slides, dried, and stained according to the immunofluorescence staining protocol. The sections were first washed in phosphate-buffered saline (PBS) with 0.25% Triton X-100 (PBS-T) for 5 min and then preincubated with 2% normal donkey serum in PBS-T for 30 min at room temperature. This solution was also used to dilute rabbit anti-histamine antibody (1:1000) and affinity purified mouse monoclonal antibody to tyrosine hydroxylase (TH; from Abcam, Germany, 1:500). The antibody solution was applied to the sections for 12–16 h at 4°C. After washing, sections were incubated with Alexa Fluor 488-labelled donkey anti-mouse IgG to reveal TH immunoreactivity in combination with cy3 donkey anti-rabbit IgG (Dianova, Hamburg, Germany) to reveal histamine immunoreactivities for 90 min at room temperature. Two negative controls (single stainings) were performed in each experiment, where one of the primary antibodies was replaced with the normal serum and further incubation with both secondary antibodies was performed as usual. Biocytin and peripherin (rabbit polyclonal antibody to peripherin, Chemicon/Millipore, 1:1000) colocalization was used for the identification of histaminergic neurons in histidine decarboxylase (HDC) knock-out (KO) and wild-type (WT) mice. For the tissue fixation in these experiments and for the staining with Dopa decarboxylase (DDC)/HDC antibodies we used paraformaldehyde (4% in 0.1 M PB). Secondary antibodies used here were Neutravidin Texas Red and Alexa Fluor 488-labelled donkey anti-rabbit IgG (Dianova). Rabbit polyclonal antibody to Dopa decarboxylase (GeneTex, Inc., Irvine, CA, USA, GTX30448) and histminergic marker (guinea pig polyclonal antibody to HDC, Acris, Bad Nauheim, Germany, 1:1000) double staining was revealed with Alexa Fluor 488- labelled goat anti-guinea pig IgG and cy3 donkey anti-rabbit IgG. For the dopamine/histamine co-localization analysis, brain slices were fixed overnight in EDAC buffer (see above) and postfixed in 0.1 M cacodylate buffer containing 10 g l^{-1} sodium metabisulfite (pH 6.2) for 15 min followed by 15 min in cacodylate/sodium metabisulfite with 0.1% glutaraldehyde (pH 7.5). After four soft washes with solution C (0.005 M Tris with 8.5 g l^{-1} sodium metabisulfite, pH 7.5), slices (350 μm) were submerged in sucrose (20%) solution and cryosectioned in 25 μm slices. Floating sections were incubated overnight with mouse anti-dopamine antibody (1:500) and rabbit anti-histamine (1:1000) antibody diluted in solution C, containing normal donkey serum 2% and Triton X-100 0.1%. Secondary antibodies (1:500), prepared on solution C were applied next day for 90 min after 3 washes with solution C. Three washes (15 min each) with solution C terminated the incubation and the sections were mounted on glass slides. Stainings were analysed with conventional fluorescence microscopy or with confocal microscopy as in Sergeeva *et al.* (2010).

Single-cell RT-PCR

Acutely isolated hypothalamic neurons were prepared from the brain slices of 25- to 28-day-old male Wistar rats ($n = 6$) as previously described (Parmentier *et al.* 2009). Whole-cell patch-clamp recordings in voltage clamp mode were used to determine the electrophysiological properties and viability of the neurons, which responded with sodium current to depolarizing voltage steps. After recording, the cytoplasm of the cell was sucked into the electrode in a stream of sterile control solution. The content of the electrode (8 μl) was expelled into an Eppendorf tube, containing 7 μl of a mixture prepared according to the protocol of the 'first strand cDNA synthesis kit' (Pharmacia Biotech, Freiburg, Germany). After incubation for 1 h at 37°C for reverse transcription (RT) this reaction was stopped by freezing at −20°C. Three negative controls were run on each day of neuronal harvesting (for details see Sergeeva *et al.* 2002). In addition the cytoplasm of three to six neurons was harvested and processed for the PCR without reverse transcription. In none of those cells were dopamine receptor transcripts detected.

Cell identification was performed by histidine decarboxylase (HDC)-cDNA amplification as previously described (Sergeeva *et al.* 2002), which generated PCR products of 457 b.p. size. Transcripts of additional markers of histaminergic neurons such as vesicular monoamine transporter type 2 (VMAT2) and peripherin (Prph) (Eriksson *et al.* 2008) were amplified in the first amplification round with primers (matching rat and mouse cDNA sequences): Prph up (5′-AGA AGA AAC (T/C)CG CA GCG GGA-3′) and Prph lo (5′-GAGC GTA GGG CCT CAT GGT TG-3′), and VMAT2up (5′-TTT TGG GAT ACT TGC ACA CAA AAT-3′) and VMAT2lo (5′-TGG ACA TTA TTC TGA GTG TAC ATC TTT-3′). In the second amplification round VMAT2up was taken with VMAT2lo2 (5′-GCA CCA CCA GCA GAG GG-3′), generating PCR product of 285 b.p. size, and Prph up was taken with Prph lo2 (5′-CGA TGT TCT C(AG)T ACT GTG CAC GG-3′), generating 275 b.p. amplimer. Encoding for the Dopa decarboxylase (DDC) cDNA was amplified in the

first amplification round with primers DDCup (5′-CTG CAG GCT TAC AT(TC) CGA A-3′) and DDClo (5′-TTG ATC TCT GAA GCA GCT-3′); in the second amplification round DDCup was taken in combination with DDClo2 (5′-GCC CTC AGC ACA CTG CT-3′), yielding PCR products of 311 b.p. size.

In a first amplification round for the dopamine 1–4 receptor cDNA primers Dop Dg up (5′-(AT) (GC)C AT(CT) (CT)T(GC) AA(CT) CT(GC) TG(CT)-3′), Dop1lo (5′-ATT ACA GTC GTT GGA GAT GGA GCC-3′), D2lo (5′-TCT GCG GCT CAT CGT CTT AAG-3′), D3lo2 (5′-TGG GTG TCT CAA GGC AGT GTC T-3′), and D4lo (5′-TGT GAA GCT TGG TGT GCC-3′) primers were taken together. In a second amplification round primers following subtype-specific primer pairs were taken in separate reactions: Dop1up (5′-GAC AAC TGT GAC ACA AGG TTG AGC-3′) and Dop1lo2 (5′-CTG GCA ATT CTT GGC ATG GAC TG-3′), generating product of 177 b.p. size; D2up (5′-GCA GTCC GAG CTT TCA GAG CC-3′) and Dop2lo2 (5′-GCT ATA CCG GGT CCT CTC TGG-3′), generating PCR products of 119 b.p. (short) and 206 b.p. (long) size; D3up2 (5′-CAT CCC ATT CGG CAG TTT TCA A-3) and D3lo2 (see above) generating PCR product of 200 b.p. size; D4up2 (5′-GTG TGC GGC CTC AAT GAT GT-3′) and D4lo2 (5′-GCC GCA AGC CAC GGA-3′), generating product of 151 b.p. size. Primers for the first amplification round for the D5 cDNA were D5up (5′-AGA AGG GAG GAC GGA GAA CTG-3′) and D5lo (5′-TCG GCA TCC CCA CTA CTG CA-3′). In the second amplification round D5lo primer was taken in combination with D5up2 (5′-AGT CGT GGA GCC TAT GAA CCT GAC-3′), generating product of 164 b.p. size.

PCR products (positive control or selected single-cell derived cDNAs used as a template) obtained after two amplification rounds were purified in water and sequenced. The obtained sequences corresponded to the known one for the rat (GENBANK, accession number): VMAT2 (NM013031), Peripherin (AF031878); D2 receptor (U22830), D1 receptor (M35077), D3 receptor (X53944), D4 receptor (M84009) and D5 (former D1B) receptor (M69118) cDNAs. Thin-walled PCR tubes contained a mixture of first strand cDNA template (1–1.5 μl), 10× PCR buffer, 10 pM each of sense and antisense primer, 200 μM of each dNTP and 2.5 units Taq polymerase. The final reaction volume was adjusted to 10 μl with nuclease-free water (Promega, Mannheim, Germany). The magnesium concentration was 3 mM in all PCR reactions. The Taq enzyme, PCR buffer, Mg^{2+} solution, and four dNTPs were all purchased from Qiagen (Erkrath, Germany). All oligonucleotides were synthesized by MWG-Biotech (Ebersberg, Germany). Amplification was performed on a thermal cycler (Mastercycler, Eppendorf, Germany). A two round amplification strategy was used in each protocol. In each round 35 cycles of the following thermal programmes were used: denaturation at 94°C for 48 s, annealing at 53°C for 48 s, and extension at 72°C for 1 min. For the second amplification round, 1 μl of the product of the first PCR was used as a template. Products were visualized by staining with ethidium bromide and analysed by electrophoresis in 2% agarose gels.

Real-time RT-PCR analysis of gene expression in HDC KO and WT mice

Total cellular mRNA was isolated from posterior hypothalamic slices using an mRNA isolation kit (Pharmacia Biotech) from 6- to 11-week-old KO ($n = 4$) and WT ($n = 4$) mice according to the manufacturer's protocol. Total mRNA was eluted from the matrix with 200 μl of RNase-free water. For the reverse transcription, 8 μl of eluted mRNA was added to 7 μl of reagents mixture prepared according to the protocol of the 'first strand cDNA synthesis kit' (Pharmacia Biotech). After incubation for 1 h at 37°C the reverse transcription reaction was stopped by freezing at –20°C. The reverse transcription reactions were not normalized to contain the equivalent amounts of total mRNA. The PCR was performed in a PE Biosystems GeneAmp 5700 sequence detection system using the SYBR green master mix kit. Each reaction contained 2.5 μl of the 10× SYBR green buffer, 200 nM dATP, dGTP and dCTP and 400 nM dUTP, 2 mM MgCl2, 0.25 units of uracil *N*-glycosylase, 0.625 units of Amplitaq Gold DNA polymerase, 10 pM forward and reverse primers, 5 μl of 1:4 diluted cDNA, and water to 25 μl. All reactions were normalized on β-actin expression, which was amplified with the primers β-actin up: 5′-CGT GAA AAG ATG ACC CAG ATC ATG TT-3′; β-actin lo: 5′-GCT CAT TGC CGA TAG TGA TGA CCT G-3′. Primers for the markers of histaminergic neurons such as peripherin, VMAT2 and for the dopamine receptors were the same as for the single-cell RT-PCR (see above), but modified to avoid mismatches with mouse cDNA sequences: VMAT2up2 and VMAT2lo; Prph up and Prph lo2, DDCup and DDClo2; Dop2lo2 and D2up, Dop1up and Dop1lo2, D3up2 and D3lo2. D4 and D5 receptor transcripts were not detected in a sufficient amount from mouse TMN cDNA amplification to be reliably quantified after one amplification round. Encoding for the dopamine transporter cDNAs were amplified with the following primers: DATup: 5′-ATC ATT GCC ACA TCC TCC AT-3′ and DATlo: 5′-CAT ATG GCA AAA GGG GAC TG-3′.

The reactions were performed in optical tubes capped with MicroAmp optical caps. The reactions were incubated at 50°C for 2 min to activate uracil *N*′-glycosylase and then for 10 min at 95°C to inactivate the uracil *N*′-glycosylase and activate the Amplitaq Gold polymerase followed by 40 cycles of 15 s at 95°C, 1 min at 60°C. The PCR reactions were subjected to a heat

dissociation protocol (PE Biosystems 5700 software). Following the final cycle of the PCR, the reactions were heat denaturated over a 35°C temperature gradient at 0.03°C s^{-1} from 60 to 95°C. Each PCR product showed a single peak in the denaturation curves. Standard curves for real-time PCR protocols with all primer pairs obtained with sequential dilutions of one cDNA sample (till 1:128) were found optimal (linear regression coefficients were >0.95). Semiquantitative analysis of receptor or cellular marker expression relative to the β-actin endogenous control was performed according to the '$2^{-\Delta\Delta C_t}$' (ΔFold) method as described previously (Sergeeva *et al.* 2003). The non-parametrical Mann-Whitney *U* test was used for the comparison between averages (6–9 data points for each animal). Selected real-time PCR products were purified in water and sequenced. The obtained sequences corresponded to the known one for the mouse (GENBANK, accession number): VMAT2 (BC078449), Peripherin (BC046291), D2 receptor (X55674), D1 receptor (BC137641), D3 receptor (BC137819), Dopa decarboxylase (NM_016672), DAT (AF109072).

Surgery, polygraphic recording in the mouse and analysis of sleep-wake parameters

All experiments followed EEC (86/609/EEC) directives. At the age of 12 weeks and with a body weight of 30 ± 2 g, HDC KO and WT mice used for electroencephalogram (EEG) and sleep–wake studies were chronically implanted, under deep gas anaesthesia using isoflurane (2%, 200 ml min^{-1}) and a TEM anaesthesia system (Bordeaux, France), with six cortical electrodes (gold-plated tinned copper wire, Ø = 0.4 mm, Filotex, Draveil, France) and three neck muscle electrodes (fluorocarbon-coated gold-plated stainless steel wire, Ø = 0.03 mm, Cooner Wire, Chatsworth, CA, USA) to record the EEG) and electromyogram (EMG) and to monitor the sleep-wake cycle. Finally, the electrode assembly was anchored and fixed to the skull with Super-Bond (Sun Medical Co., Shiga, Japan) and dental cement. This implantation allows stable and long-lasting polygraphic recordings.

After surgery, the animals were housed individually in barrels placed in an insulated sound-proof recording room maintained at an ambient temperature of 22 ± 1°C and on a 12 h light–dark cycle (lights on at 07.00 h), standard food and water being available *ad libitum*. After a 7 days recovery period, mice were habituated to the recording cable for 7 days before polygraphic recordings were started. Cortical EEG (contralateral frontoparietal leads) and EMG signals were amplified, digitized with a resolution of 256 and 128 Hz, respectively, and computed on a CED 1401 Plus (Cambridge Electronic Design, Cambridge, UK). Using a Spike2 script and with the assistance of spectral analysis using the fast Fourier transform, polygraphic records were visually scored by 30 s epochs for wakefulness (W), slow wave sleep (SWS), and paradoxical sleep (PS) according to previously described criteria validated for mice (Parmentier *et al.* 2002, 2009).

Animals were subjected to 12 h sleep–wake recordings following administration of freshly prepared vehicle or quinpirole, either by an intraperitoneal (I.P.) or an oral route at 10.00 h, i.e. during the sleepy period. The vehicle consisted of 0.05 ml of 0.9% NaCl alone (for the I.P. route) or containing methylcellulose at 1% (for the oral route). Oral application was performed using a mouse oral administration probe (20G, Phymep, Paris). Statistical analysis was performed with Dunnett's test and ANOVA for repeated measures. Significance level was set at $P < 0.05$. Data are presented as means ± standard error of the mean (SEM).

Drugs

Quinpirole, sulpiride, (*R*)-(–)-α-methylhistamine dohydrobromide, U73122, 6,7-dinitroquinoxaline-2,3-dione disodium salt (DNQX); 6-cyano-7-nitroquinoxaline-2,3-dione disodium salt (CNQX), D-(–)-2-amino-5-phosphonopentanoic acid (D-AP5), 2-(4-morpholinyl)-8-phenyl-4*H*-1-benzopyran-4-one hydrochloride (LY294002), N^G-nitro-L-arginine methyl ester hydrochloride (L-NAME), 2-methyl-6-(phenylethynyl)pyridine hydrochloride (MPEP), 1-[2-(4-methoxyphenyl)-2-[3-(4-methoxyphenyl)propoxy]ethyl-1*H*-imidazole hydrochloride (SKF 96365), (±)-1-phenyl-2,3,4,5-tetrahydro-(1*H*)-3-benzazepine-7,8-diol hydrobromide (SKF 38393), (*S*)-(+)-α-amino-4-carboxy-2-methylbenzeneacetic acid (LY 367385), 3-[[4-(4-chlorophenyl)piperazin-1-yl]methyl]-1*H*-pyrrolo[2,3-b]pyridine trihydrochloride (L-745,870) and *N*-(methyl-4-(2-cyanophenyl)piperazinyl-3-methylbenzamide maleate (PD168077) were obtained from Tocris (Biozol, Eching, Germany). Reactive blue 2 (cibacron blue), *N*-methyl-D-glucamine (NMDG), benzamil hydrochloride hydrate, dopamine hydrochloride, L-3,4-dihydroxyphenylalanine methyl ester hydrochloride (laevodopa or L-Dopa), forskolin, *N*-[2-(*p*-bromocinnamylamino) ethyl]-5-isoquinoline sulfonamide (H-89), tetrodotoxin, nomifensine maleate salt, picrotoxin, CGP55845 and gabazine (SR-95531) were obtained from Sigma/RBI (Deisenhofen, Germany).

Results

L-Dopa excites TMN neurons in rat brain slices

When applied to the dopaminergic neurons of the substantia nigra, L-Dopa (100 μM) causes release of dopamine and activation of D2-like receptors (Mercuri *et al.* 1990;

Sebastianelli *et al.* 2008), which demands uptake of L-Dopa into neurons through the L-amino-acid transporter and conversion into dopamine. L-Dopa (100 μM) increased the firing rate of TMN neurons to 148 ± 22% ($n = 5$) of control. Preincubation with 5 mM L-histidine, which competes with L-Dopa for the L-amino-acid transporter, abolished the effect of L-Dopa ($n = 6$, Fig. 1*A*); D-histidine was inactive ($n = 3$). Excitation of TMN neurons by L-Dopa was blocked by antagonists at D2R (sulpiride, 10 μM) and D1/D5R (SCH 39166, 1 μM) ($n = 5$, Fig. 1*B*, lower panel). For the construction of the dose–response curve for L-Dopa, only neurons with strong excitation (more than 29% increase in firing rate over control) were selected (13 out of 20 investigated cells). Half-maximal increase in firing rate was observed at 15.4 ± 5 μM (Fig. 1*C*). The firing rate of TMN neurons was increased in these experiments from 1.2 ± 0.25 Hz in control to 2.6 ± 0.6 Hz under 100 or 300 μM of L-Dopa (226%).

Expression of Dopa decarboxylase, VMAT2 and dopamine receptors in rat TMN neurons

The electrophysiological data described above were unexpected as only low mRNA levels for the D1- and D2-like receptors as well as weak receptor binding have been reported for the lateral hypothalamus (Mansour *et al.* 1990) and the location (neuronal *vs.* glial) of these receptors remained unclear. Acutely isolated TMN neurons were now subjected to single-cell RT-PCR analysis of histaminergic markers (HDC, peripherin, vesicular monoamine transporter 2 (VMAT2)), Dopa decarboxylase and five known dopamine receptors. The majority of HDC-positive cells ($n = 29$) expressed peripherin (86%) and VMAT2 (79%). All five dopamine receptors were variably expressed in TMN neurons. The D2L but not the D2S splice variant was detected in TMN neurons (Fig. 1*D*). Three non-histaminergic cells characterized by high levels of DDC expressed D2S transcripts. DDC amplimers were sequenced from three highly positive TMN cells, but the remaining histaminergic cells were not clearly positive, indicating either no or low expression. Immunostainings revealed that Dopa decarboxylase (DDC, also called aromatic amino acid decarboxylase AADC) is co-localized to a large degree with the histaminergic cell marker HDC in TMNv (Fig. 1*E*).

Localization of dopaergic and histaminergic neurons in the posterior hypothalamus of the rat

What is the natural source of L-Dopa for the TMN neurons which are negative for tyrosine hydroxylase (TH, L-Dopa producing enzyme) in developing rat brain (Vanhala *et al.* 1994) as well as in young adults (present study)? L-Dopa is produced in the brain by dopaminergic, noradrenergic and adrenergic cells and may be released and taken up by other cells, which express Dopa decarboxylase and therefore are able to produce dopamine. Interestingly, a large fraction of hypothalamic dopaminergic neurons are not dopaergic and vice versa (Zoli *et al.* 1993; Weihe *et al.* 2006). Coronal and horizontal rat brain slices containing the TMN (Fig. 2) were co-stained for histamine and tyrosine hydroxylase. TH immunoreactivity was not found in the ventral TMN (TMNv, Fig. 2*A*, right image) the site of our recordings, but TH-positive cells and fibres were seen in close proximity to TMN neurons in adjacent regions (Fig. 2*A*, left, *B*, *C* and *D*) such as the supramamillary nucleus, ventral premamillary nucleus and posterior periventricular nucleus. Previous studies have shown that midbrain dopaminergic neurons from substantia nigra compacta (SNc) and from VTA do not project to the TMN (Arbuthnott & Wright, 1982; Swanson, 1982). Thus, the natural source for L-Dopa for the TMNv neurons (recording site) may be located within the hypothalamus or at remote sites (substantia nigra or striatum) where they send dense projections.

Histaminergic neurons are activated by dopaminergic agonists

Rat ventrolateral TMN neurons responded to dopamine (100 μM), quinpirole (D2-like receptor agonist, 10–100 μM) and SKF 38393 (85 μM, D1/D5-agonist) with an increase in firing rate (Fig. 3*A*–*C*). As active concentrations of dopaminergic agonists exceeded their normally used concentrations 5–10 times, we suspected first the involvement of excitatory or inhibitory gliotransmitters or other neurotransmitters in their action. Maximal responses in glial cells can only be evoked by concentrations of quinpirole higher than 50 μM due to the low level of dopamine receptor expression (Khan *et al.* 2001; Li *et al.* 2006). Neither glutamate receptor blockers, nor the P2Y receptor blocker Cibacron Blue (10 μM) in association with antagonists at mGluR1 LY 367385 (20 μM) and mGluR5 MPEP (10 μM) nor the inhibitor of nitric oxide synthesis L-NAME (200 μM) or the phosphatidylinositol 3-kinase inhibitor LY294002 (10 μM) significantly affected the quinpirole (100 μM)-induced response. Block of $GABA_A$, $GABA_C$, and glycine receptors and other chloride channels by picrotoxin (100 μM) increased the firing of TMN neurons from 1.7 ± 0.5 Hz in control to 3 ± 0.4 Hz ($n = 6$), but the excitatory action of quinpirole remained unchanged (Fig. 3*D*). The $GABA_B$ receptor antagonist CGP55845 was also ineffective against quinpirole excitation (Fig. 3*D*). The effect of quinpirole was abolished at room temperature (Fig. 3*D*), indicating involvement of temperature-dependent exchange or transport, as previously described for the serotonin 2C receptor

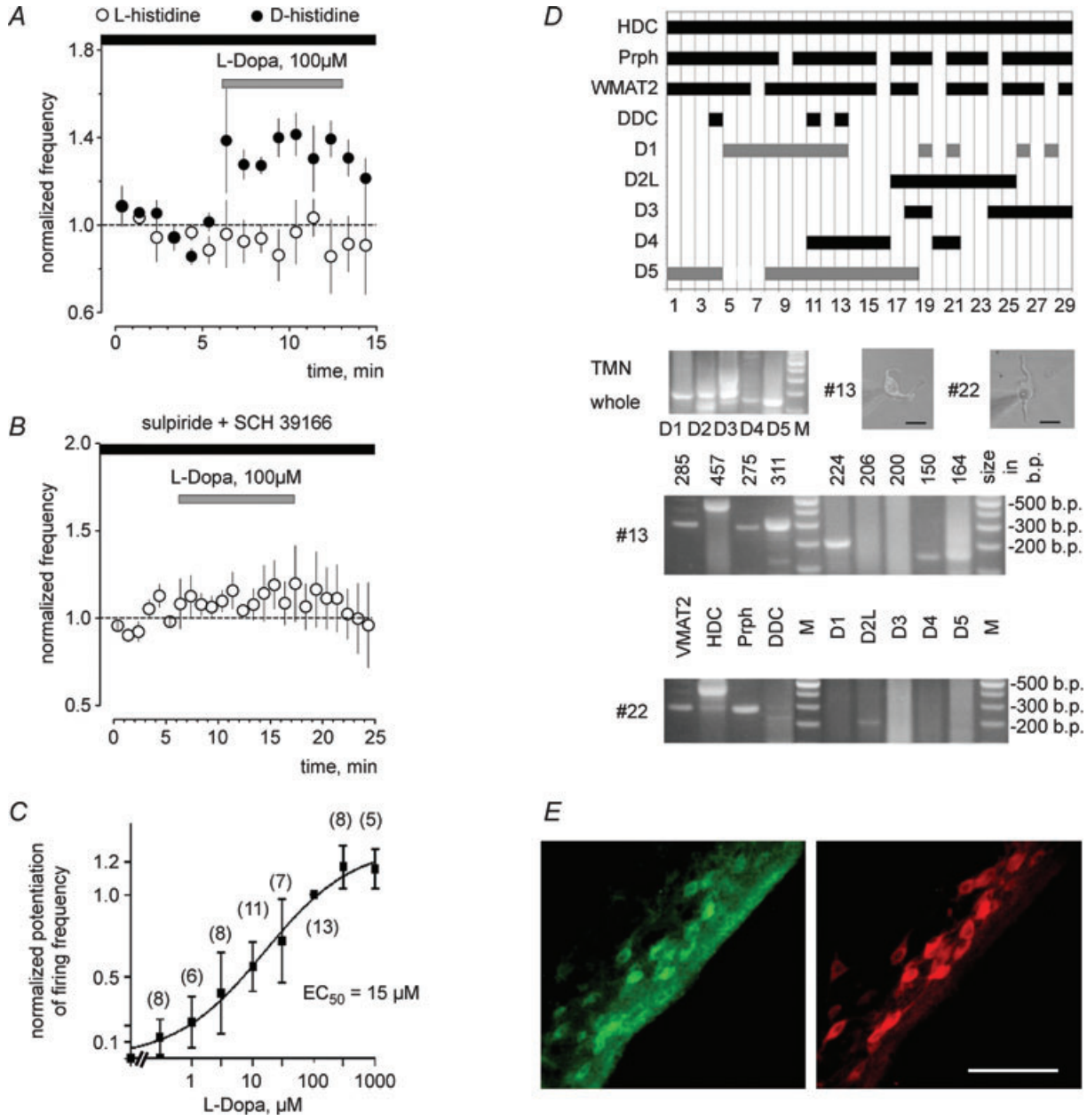

Figure 1. TMN histaminergic neurons are excited by L-Dopa, express dopamine (D) receptors and Dopa decarboxylase

A, excitatory action of L-Dopa depends on L-amino acid uptake and can be blanked by the preincubation with L-histidine, but not with D-histidine. *B*, effect of L-Dopa is abolished by the combined application of D1/5 and D2-like receptor antagonists. *C*, L-Dopa dose–response curve fitting with the Hill equation yielded $EC_{50} = 15.4 \pm 5$ μM, Hill coefficient (n_H) $= 0.6 \pm 0.7$. Potentiation of firing frequency over the control level was normalized on potentiation by 100 μM of L-Dopa. Number of cells tested with each concentration is given in brackets. *D*, floating bar histogram illustrating co-localization of histaminergic markers: histidine decarboxylase (HDC), vesicular monoamine transporter 2 (VMAT2), peripherin (Prph), the dopaminergic marker Dopa decarboxylase (DDC) and 5 dopamine receptors (D2L for long splice variant) in 29 TMN neurons (single-cell RT-PCR). Digital images of two neurons (scale bar 20 μm) and corresponding gels documenting RT-PCR analysis of dopamine receptor expression as well as cellular markers in these neurons (no. 13 and no. 22) and in positive control (TMN whole) are given below. M: DNA size marker (100 b.p. ladder). Expected size of PCR products is given above the upper gel. *E*, co-localization of DDC (AF488, green) with histidine decarboxylase (cy3, red) in rat TMN. Scale bar 100 μm.

action (Eriksson *et al.* 2001*a*) or orexin-receptor action (Eriksson *et al.* 2001*b*) in TMN neurons. The action of quinpirole was blocked by inhibitors of phospholipase C (PLC) U73122 and of the Na^+/Ca^{2+} exchanger benzamil (Fig. 3*D*), but was unchanged in the presence of the $\alpha1/\alpha2$ adrenoreceptor blocker prazosine (20 μM) or in the presence of the dopamine uptake inhibitor nomifensine (1 μM). The activator of cAMP and PKA forskolin (10 μM) increased the firing frequency of TMN neurons to $256 \pm 46\%$ of control ($n = 12$). Quinpirole given after a plateau response was achieved under forskolin exerted a further significant increase in firing frequency ($13 \pm 3\%$ over control, $n = 4$, $P < 0.001$). The protein kinase A inhibitor H-89 (10 μM) did not affect the quinpirole excitation (Fig. 3*D*). Dose–response curves for quinpirole were obtained from firing rates. The half-maximal concentration of quinpirole calculated from the dose–response curve was 47 μM (Fig. 4*A*).

In whole-cell current clamp recordings, quinpirole (100 μM) depolarized TMN neurons by 3.8 ± 0.3 mV ($n = 5$, Fig. 4*B*). This depolarization (4.1 ± 0.4 mV, $n = 6$) was also present under TTX (1 μM), CNQX (5 μM), D-AP5 (50 μM) and gabazine (10 μM). In voltage-clamp experiments ($V_{hold} = -70$ mV) quinpirole evoked an inward current of 55 ± 13 pA (ranging from -24 pA to -104 pA; $n = 6$; Fig. 4*C*) that was accompanied by a decrease in membrane resistance to $83 \pm 4\%$ of control ($n = 6$; $P = 0.0470$, paired t test). During TRPC (transient receptor potential canonical) channel block by SKF 93635 (25 μM), the quinpirole-induced inward current was significantly reduced (-19 ± 4 pA, $n = 5$ cells; $P = 0.035$; Fig. 4*C*), whereas no current was induced

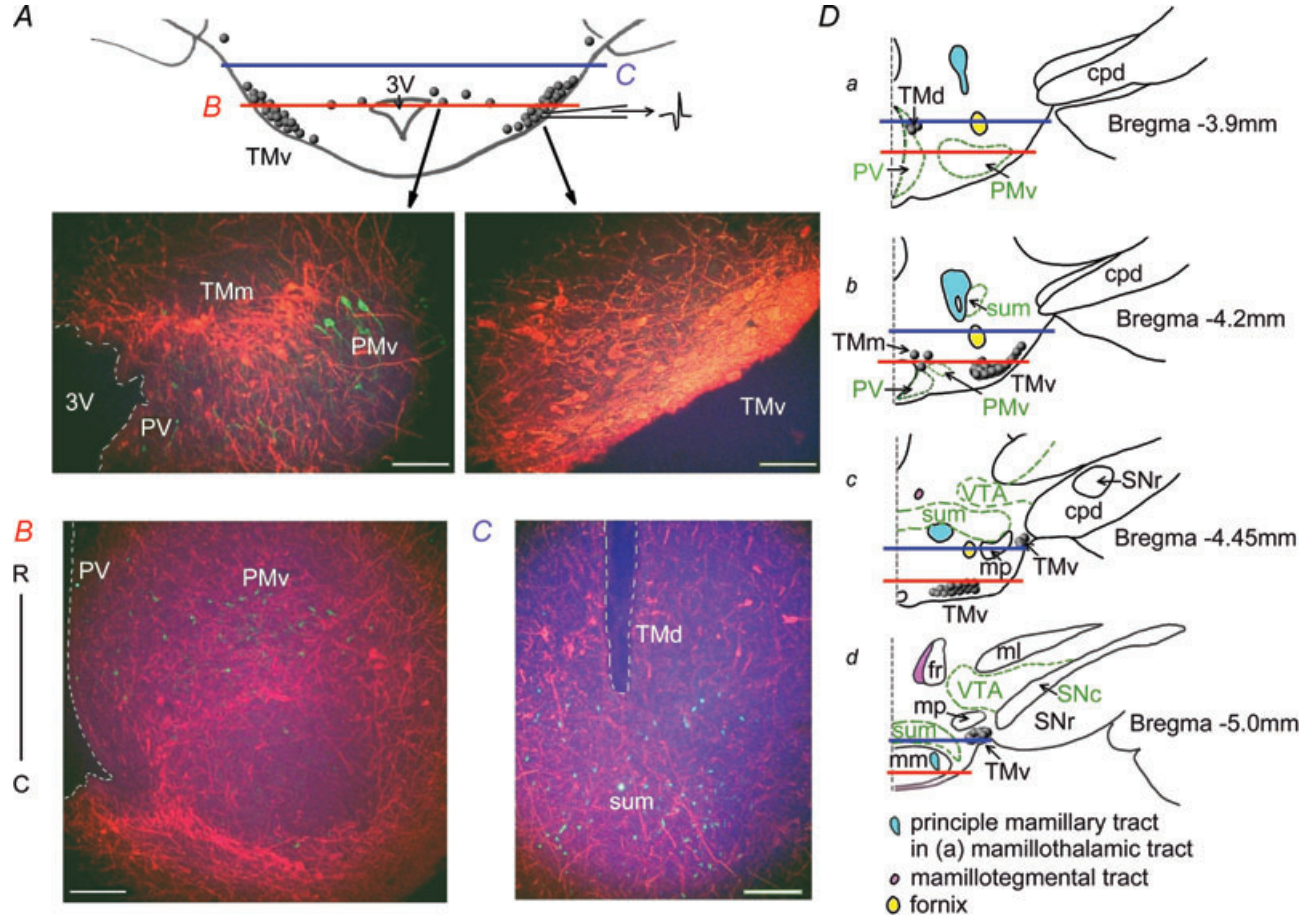

Figure 2. Co-localization of tyrosine hydroxylase- and histamine-containing neurons in the posterior hypothalamus
A, coronal rat (P25) brain slice as used for the electrophysiological recordings from ventral TMN (TMv). 3V: third ventricle. *B* and *C*, two levels of horizontal slice sections (R-C for rostro-caudal axis) are indicated with red and blue lines. Double immunostaining for histamine (revealed with cy3, red) and tyrosine hydroxylase (TH, revealed with AF488, green). White dotted line indicates location of third ventricle. Scale bar: 200 μm. *D*, schematic presentation of coronal sections containing TMN (TMd-TMN dorsal; TMv-TMN ventral; TMm-TMN medial, adopted from the Atlas of Swanson (1992). Areas containing dopaminergic/dopaergic cells are marked green. Abbreviations: cpd, cerebral peduncle; fr, fasciculus retroflexus; ml, medial lemniscus; mm, medial mamillary nucleus; mp, mamillary peduncle; PV, posterior periventricular nucleus of hypothalamus; PMv, ventral premamillary nucleus; VTA, ventral tegmental area; SNc, substantia nigra compacta; SNr, substantia nigra reticulata; sum, supramamillary nucleus.

by quinpirole after replacement of extracellular NaCl with an equimolar concentration of NMDG ($n = 4$). Current–voltage relationships obtained by applying slow voltage ramps either in control or in the presence of quinpirole (100 μM) showed a rightward shift of the *I–V* curve induced by quinpirole, which was absent in experiments with NMDG. Calculated net current reversed its polarity at -5.3 ± 0.6 mV (Fig. 4*D*).

Quinpirole increases GABAergic inhibition

Under control conditions mIPSC frequency and amplitude recorded from five rat TMN neurons in slices were 3.3 ± 0.1 Hz and 26 ± 4 pA, respectively. Quinpirole (100 μM) increased the frequency of mIPSCs by 52% (Kolmogorov–Smirnov two-sample test applied to the cumulative fraction histograms as shown in Fig. 5*A* indicated a significant difference between inter-event intervals in control and under quinpirole $P < 0.005$, $n = 5$). The increase in mIPSCs frequency did not recover to the control level after quinpirole withdrawal (Fig. 5*B*), like the firing frequency of TMN neurons (Fig. 3*C*). There were no significant changes in mIPSC amplitudes and decay times under quinpirole (27 ± 6 pA, 26 ± 4 ms).

Quinpirole increases histamine release from the TMN of freely moving rats

After collection of four 15 min baseline samples, quinpirole (10 μM) was infused for 60 min locally into the TMN through the dialysis probe. As shown in Fig. 5*C*, 60 min perfusion with quinpirole induced a significant increase in histamine release (ANOVA, $F_{(11,56)} = 2.003$,

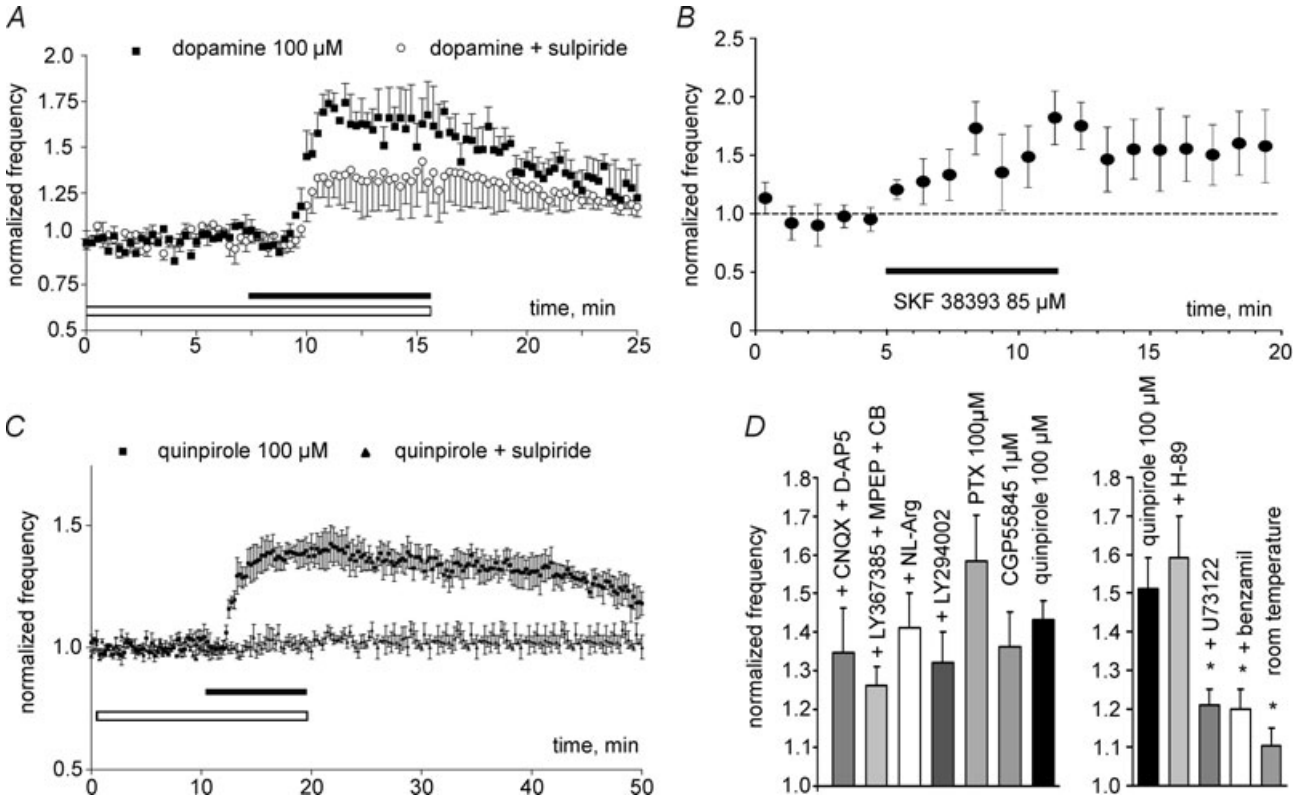

Figure 3. Dopaminergic excitation of TMN histaminergic neurons
A, dopamine excites rat TMN neurons ($n = 5$), and the effect is partially blocked by the D2-selective antagonist sulpiride ($n = 4$). *B*, the D1/5 dopamine receptor type agonist SKF 38393 increases the firing rate of TMN neurons ($n = 6$). *C*, quinpirole (100 μM) increases firing frequency in TMN neurons ($n = 12$). Sulpiride abolishes the action of quinpirole ($n = 4$). *D*, left graph, increase in firing rate of TMN neurons is independent of glutamate, ATP/ADP, growth hormones (IP_3-dependent signalling) and nitric oxide (possible messengers of glia–neuron signalling). The following antagonists were used: D-AP5 (NMDA receptors), CNQX (AMPA receptors), LY367385 (mGluR1), MPEP (mGluR5), cibacron blue (broad spectrum antagonist at P2Y receptors), LY294002 (IP3-kinase inhibitor), PTX (picrotoxin), CGP 55845 ($GABA_B$ receptor antagonist) and NL-Arg (=L-NAME, NOS inhibitor). Right graph, quinpirole action is not affected by PKA inhibitor H-89 (10 μM), but significantly reduced by an inhibitor of phospholipase C (PLC), U73122 (5 μM), by the Na^+/Ca^{2+} exchanger antagonist benzamil (10 μM) and at room temperature. Four to six TMN neurons were tested with each experimental protocol, except for the pooled control experiments (quinpirole 100 μM, $n = 7$ in left graph, $n = 12$ in right graph).

$P < 0.04$). The maximal increase (53 ± 23% over control) was achieved in the fourth 15 min fraction collected after onset of the TMN perfusion with quinpirole, and histamine release was restored to control levels during subsequent TMN perfusion with control medium. The mean spontaneous release was 0.083 ± 0.006 pmol/15 min ($n = 6$). Histamine is likely to be released from the extensive arborizations of TMN neurons within this brain area (Inagaki *et al.* 1988).

The waking effect of quinpirole is impaired in histamine deficient mice

Given orally during the lights-on period quinpirole (2 mg kg^{-1}) induced biphasic sleep–wake changes in WT mice, i.e. an initial sleep-promoting and a later wake-promoting effect (Fig. 6*A*), most likely due to a progressive absorption and so an increasing bioavailability in the brain. These data are consistent with the dose-dependant sleep–wake response of quinpirole demonstrated in previous studies in the rat (Monti & Monti, 2007). While the sleep-promoting effect remained unimpaired in HDC$^{-/-}$ mice, the wake promoting effect was absent. The initial sleep-promoting effect can be explained by the low dose acting through D2 autoreceptors on dopaminergic neurons and the later wake-promoting effect by a higher concentration acting on postsynaptic D2 receptors. Quinpirole (1 mg kg^{-1}) given I.P. significantly enhanced wakefulness at the expense of slow wave sleep (SWS) and paradoxical sleep (PS) in wild-type mice (HDC$^{+/+}$). In HDC$^{-/-}$ mice quinpirole reduced waking and increased SWS (Fig. 6*B*) without affecting PS.

Dopaminergic markers, histaminergic markers and functional dopamine receptor expression in HDC$^{-/-}$ and HDC$^{+/+}$ mice

We investigated the relative occurrence of mRNAs encoding the markers of dopamine, histamine and dopamine receptors by semiquantitative real-time RT-PCR from dissected TMN tissue samples obtained from HDC$^{+/+}$ and HDC$^{-/-}$ mice. All data points in each

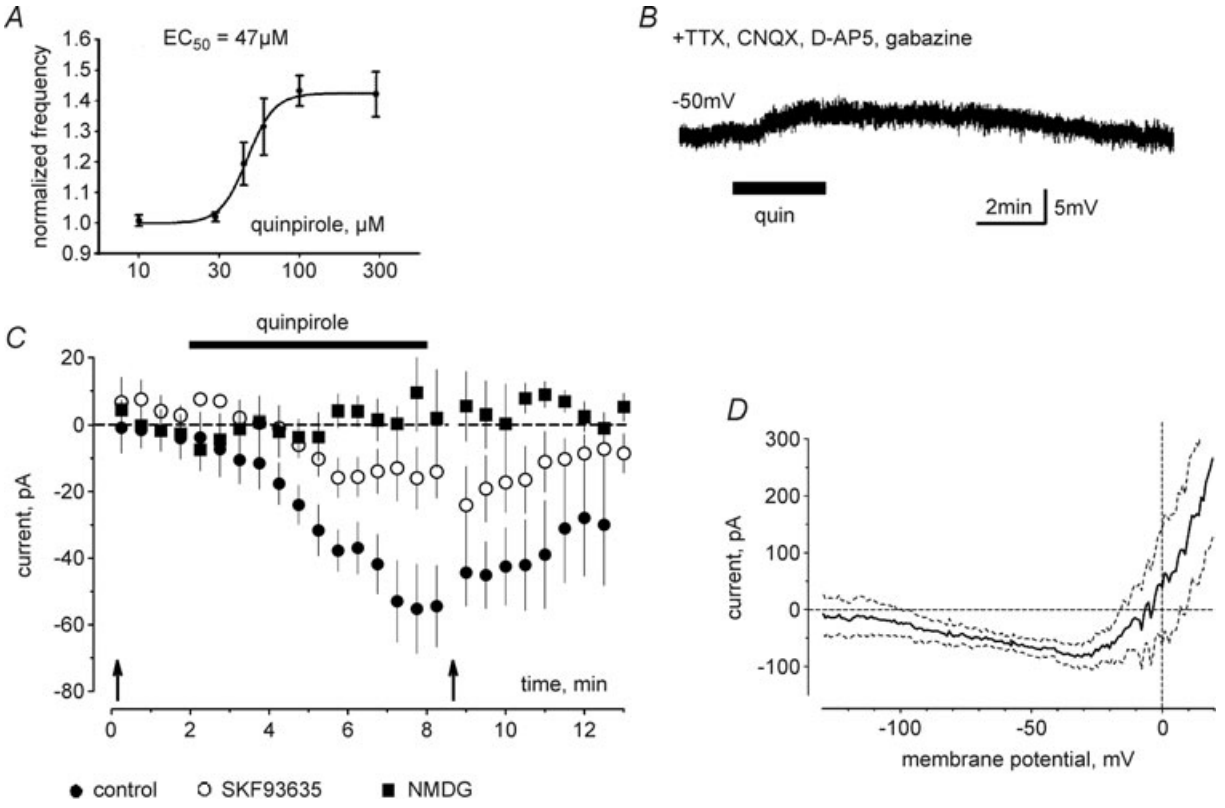

Figure 4. Dose dependence and mechanisms of quinpirole action
A, dose–response curve of quinpirole-induced increase in firing rate of TMN neurons recorded in cell-attached mode (each point is an average obtained from 4–6 neurons. *B*, quinpirole depolarizes TMN neurons recorded under TTX in whole-cell current clamp mode, indicating a direct postsynaptic effect. *C*, time course diagram for the averaged whole-cell currents recorded from TMN neurons. Replacement of Na^+ in the extracellular solution with $NMDG^+$ or appliction of the TRPC channel antagonist SKF 93635 blocked quinpirole-induced inward current. Arrows indicate application of ramps. *D*, current–voltage relationship of the quinpirole-induced net current (mean, black line ± SEM, dotted grey line, $n = 4$).

amplification were normalized to the probe with minimal level of target gene expression (Fig. 6*C*). None of the investigated genes showed differences in the expression between the two genotypes.

TMN neurons in HDC KO and WT mice were identified by regular firing and by the inhibition of firing by the H3 receptor agonist (*R*)-α-methylhistamine (0.2 μM). Quinpirole at 100 μM caused the same increase in firing in $HDC^{+/+}$ (142 ± 5% of control, $n = 13$) and in $HDC^{-/-}$ mice (145 ± 18%, $n = 8$). Five cells were successfully labelled with biocytin after recordings in cell-attached mode. In all of these cells biocytin immunoreactivity was co-localized with peripherin.

Rat TMN neurons are under an endogeneous D4R-mediated inhibitory tone

The dopamine reuptake inhibitor nomifensine increases the extracellular level of dopamine in the hypothalamus (Timmerman *et al.* 1995). Is the enhanced level of endogeneous dopamine sufficient to activate the low-affinity dopamine receptors described here? Nomifensine (1 μM) did not change the firing rate in five rat TMN neurons and suppressed firing to 64 ± 15% in six cells. In the presence of the D4 receptor antagonist L-745,870, nomifensine never caused depression in six investigated cells ($P = 0.037$, Fisher's exact probability test) (Fig. 6*D*). The D4 receptor agonist PD168077 (1 μM) suppressed the firing to 72 ± 10% ($n = 7$, $P < 0.0001$). The D4 receptor antagonist L-745,870 (1 μM) on its own increased firing of TMN neurons to 118 ± 9% of control ($n = 9$, $P = 0.036$), indicating an endogeneous inhibitory tone through the D4 receptors in rat brain slices. Neither an agonist ($n = 4$) nor an antagonist ($n = 5$) at D4 receptors changed the firing of TMN neurons in slices from mice.

Discussion

The most intriguing findings of the present study are: (i) L-Dopa is taken up by TMN neurons, converted to

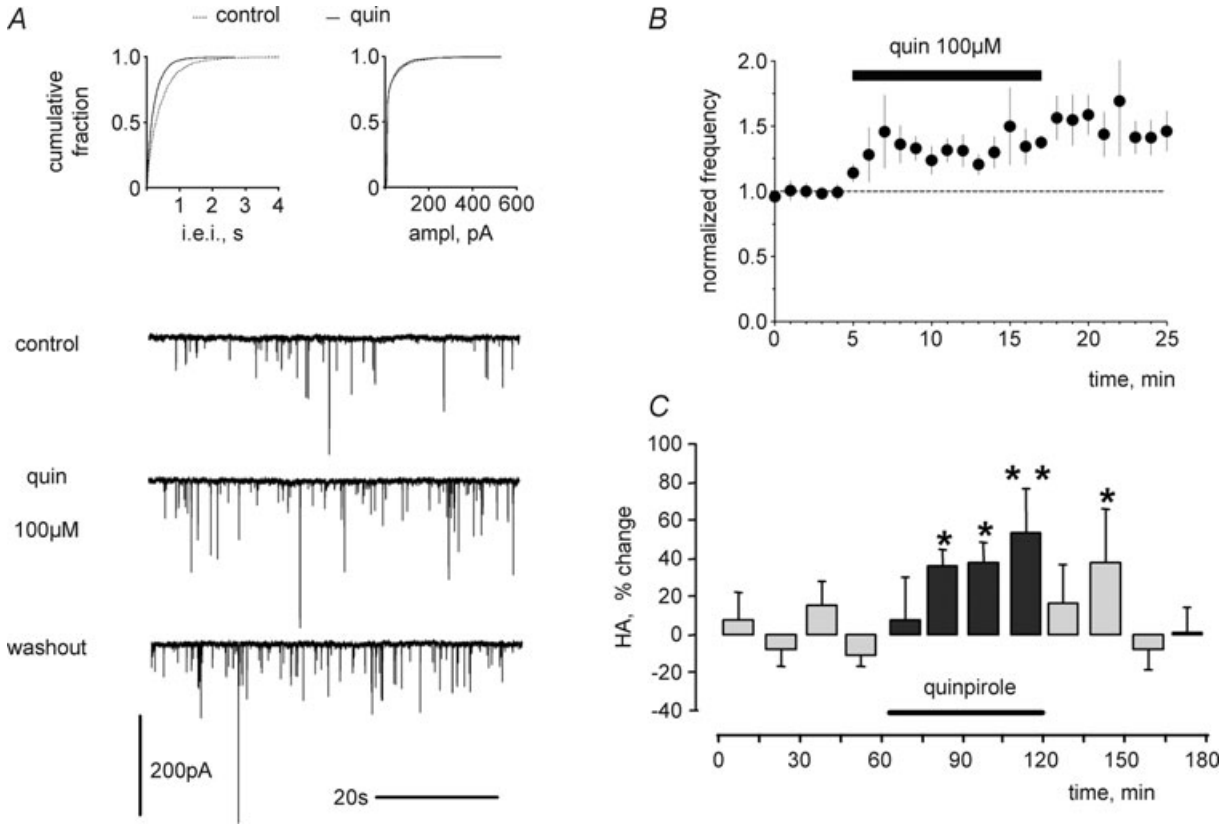

Figure 5. D2-like receptor activation increases histamine release *in vivo* in accordance with increased firing of TMN neurons despite increasing GABAergic tone in the posterior hypothalamus *in vitro*
A, quinpirole (quin) increases frequency of GABAergic mIPSCs recorded from TMN neurons in slices. Example of cumulative fraction histograms for the mIPSCs interevent interval (i.e.i) and amplitude (ampl) and corresponding original mIPSC recordings in control, under quinpirole (quin) and after drug withdrawal in one TMN neuron. *B*, time course diagram for the averaged frequency of IPSCs (normalized to the control levels, $n = 5$). *C*, quinpirole enhances histamine release in the hypothalamus, which reaches a maximal value after 1 h of administration. Shown are means ± SEM of 6 experiments normalized on the last sample before drug administration.

dopamine and released, causing excitation downstream to the D1-like and D2-like dopamine receptor activation. (ii) Histaminergic neurons express Dopa decarboxylase, the dopamine-producing enzyme, and VMAT2, the vesicular monoamine transporter 2, which accumulate dopamine and histamine in vesiscles. TMN neurons are immunopositive for dopamine and express all five types of dopamine receptors (single-cell RT-PCR). (iii) All dopamine receptors, except D4, mediate an increase of firing in TMN neurons. The D2-like receptor-mediated excitation depends on phospholipase C (PLC), transient receptor potential canonical (TRPC) channels and the Na^+/Ca^{2+} exchanger. (iv) Recordings in freely moving mice revealed a role of the histaminergic system in D2-like receptor-mediated arousal.

Thus our study identifies the histaminergic system as a novel target of dopaminergic agents (ligands at D2R, at D1/D2R and L-Dopa) used in the treatment of PD.

Two splice variants of the D2R differ in 29 amino acids, with the short isoform specifically found in dopaminergic cells as an autoreceptor, whereas the long splice variant is primarily a postsynaptic receptor in the nucleus accumbens and striatum (Khan *et al.* 1998). In keeping with these data, excitatory D2L receptors on TMN neurons (present study) do not mediate autoinhibition. Only transcripts encoding the long isoform of the D2R were detected in TMN neurons. In addition these receptors did not mediate an inhibition of adenylyl cyclase in TMN neurons that is otherwise typical for the D2-like receptors: even after maximal activation of adenylyl cyclase with forskolin (10 μM), quinpirole maintained its excitation. 'Atypically' excitatory D2-like receptors coupled to different effector systems were previously described in the supraoptic nucleus (Yang *et al.* 1991), the subthalamic nucleus (Zhu *et al.* 2002; Loucif *et al.* 2008; Ramanathan *et al.* 2008) and the serotonergic neurons of the nucleus raphe dorsalis (Haj-Dahmane, 2001). Although supraoptic nucleus neurons were depolarized by quinpirole in slices (Yang *et al.* 1991) the effects of dopamine on vasopressin secretion *in vivo* are inhibitory and most likely involve activation of GABAergic neurons. Interestingly, GAD67-positive interneurons of the dorsal lateral geniculate nucleus (dLGN) but not principle cells are excited by quinpirole in a sulpiride-sensitive way, shaping spontaneous and visually evoked activity in the dLGN *in vivo* (Munsch *et al.* 2005). The increase in frequency of GABAergic mIPSCs recorded from TMN neurons in the presence of quinpirole suggests a similar excitatory action of quinpirole on GABAergic hypothalamic neurons. Our experiments with reverse microdialysis in freely moving rats showed that quinpirole injected into the TMN enhances histamine release in the hypothalamus. Thus, the increased frequency of mIPSCs is not a decisive factor for neuronal firing and histamine release from TMN. However, a modulatory influence of GABAergic inputs is possible.

Experiments with nomifensine and a D4 antagonist demonstrated that a large fraction of TMNv neurons receives inhibitory inputs from dopaminergic (most likely hypothalamic) neurons located at a remote site; the TMNv region does not contain TH- or dopamine- positive cells or fibres. The medial and dorsal TMN subdivisions show dense mutual connections between histaminergic and hypothalamic dopaminergic cell groups such as the supramamillary nucleus, the ventral premamillary nucleus or the posterior periventricular nucleus (Fig. 2). The functional connections between histaminergic and dopaminergic or L-Dopaergic (TH-positive) cells from these regions await elucidation. DDC-positive/TH-negative neurons, which are able to produce dopamine when supplied with L-Dopa, were previously found located 0.4 mm caudal to the ventral premamillary nucleus in rats (Zoli *et al.* 1993); the transmitter identity and functional role of these nerve cells was so far unknown. Figure 2*D* demonstrates that the histaminergic TMv nucleus is located at the indicated distance caudal to PMv. We provide functional evidence that L-Dopa can be taken up through the L-amino acid transport system (competition with L-histidine) and trigger dopamine release, which excites TMN neurons through D1- and D2-like receptors (see model in Fig. 7). The majority of TMN neurons are immunopositive for Dopa decarboxylase and dopamine. Thus, we speculate, that dopamine produced in TMN significantly participates in the control of wakefulness, which would explain why orexin or histamine deficiency does not lead to major changes in the amounts of sleep and waking, but dopamine deficiency does. Activation of the histaminergic system by L-Dopa thus would lead to an increased level not only of histamine but also of dopamine in forebrain areas. Activation of H3R at an increased histamine level would reduce neuronal activity. Anti-H3R medication increases alertness in PD (Arnulf & Leu-Semenescu, 2009; Arnulf, 2009) and H3R antagonists/inverse agonists allow lowering the dosage of dopaminergic medication in PD. It was recently shown that H3Rs form heteromers either with D1 or with D2 receptors in the striatum, where histamine is able to decrease sensitivity of the resulting receptor to dopaminergic drugs, while an H3R antagonist increases its sensitivity (Sanchez-Lemus & Arias-Montano, 2004; Ferrada *et al.* 2008; Ferrada *et al.* 2009). A large body of experimental evidence shows that histamine and dopamine act reciprocally in the control of movement (Morgan *et al.* 1998). Antihistaminergic treatment suppresses apomorphine-induced turning behaviour in 6-hydroxydopamine (6-OHDA) lesioned rats (Liu *et al.* 2008). Imetit (an H3R agonist) attenuates L-Dopa-mediated release of dopamine

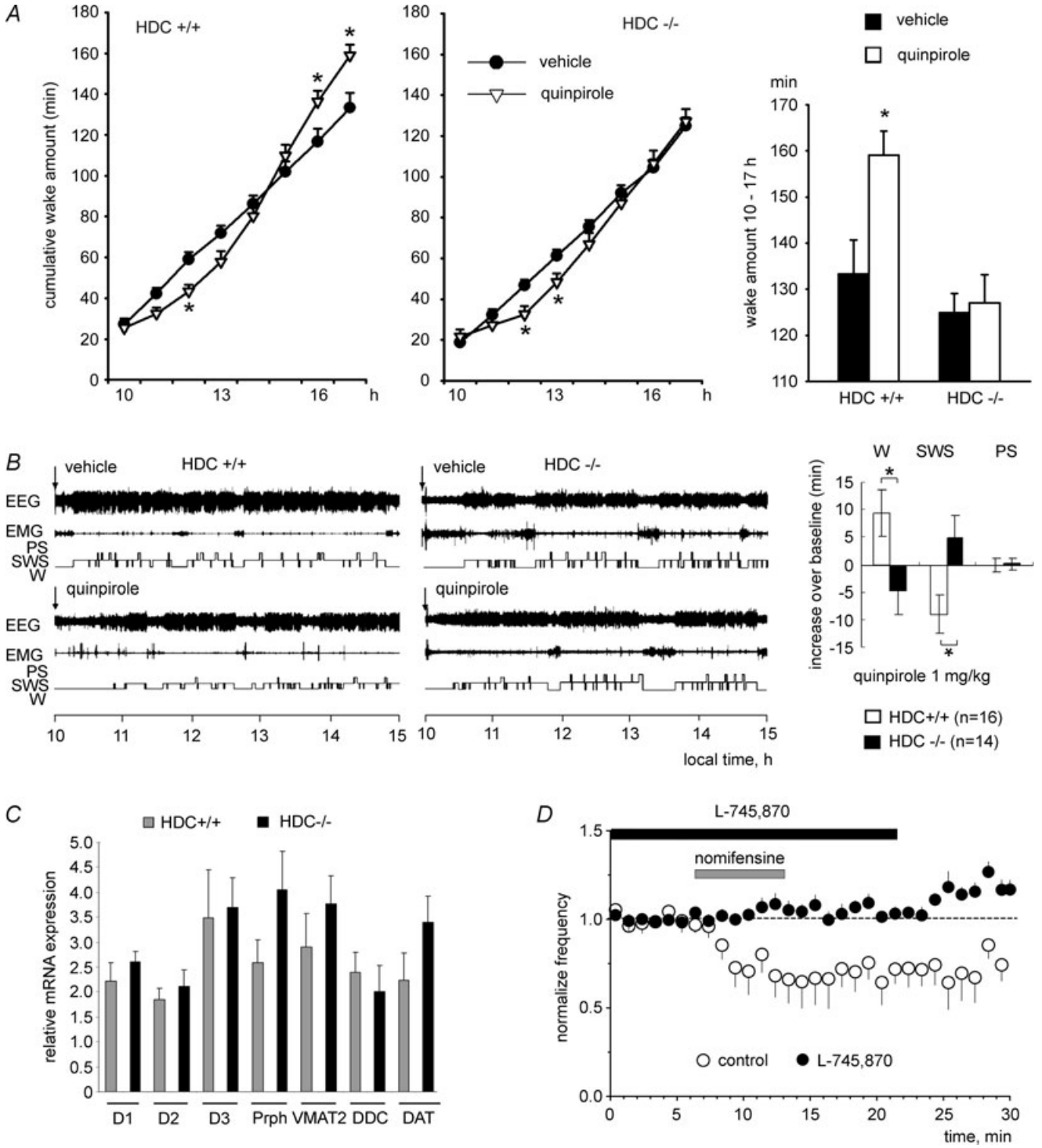

Figure 6. Quinpirole-induced arousal is partially mediated through histamine
A, histograms for the cumulative amount of waking show that HDC$^{-/-}$ mice ($n = 15$) display a similar decrease in waking during the first 3 h after quinpirole intake when compared to the WT ($n = 15$) mice but lack subsequent increase in waking. *B*, typical example of polygraphic recording and corresponding hypnograms showing the effect of systemically applied quinpirole on the cortical EEG and EMG and sleep–wake cycle, illustrating the increase in waking in HDC$^{+/+}$ ($n = 16$) and HDC$^{-/-}$ ($n = 14$) mice. The moment of injection is indicated with array. Diagram (at the right) illustrates sleep–wake changes relative to baseline for the mean values (min ± SEM) spent in each sleep–wake stage during 3 h after injection of quinpirole at 10.00 h. Note that quinpirole (1 mg kg^{-1}) causes a significant increase in waking (W) and a decrease in slow wave sleep (SWS) in WT but the opposite effects in HDC$^{-/-}$ mice. *C*, real-time RT-PCR analysis of the relative expression of transcripts of dopamine receptors and

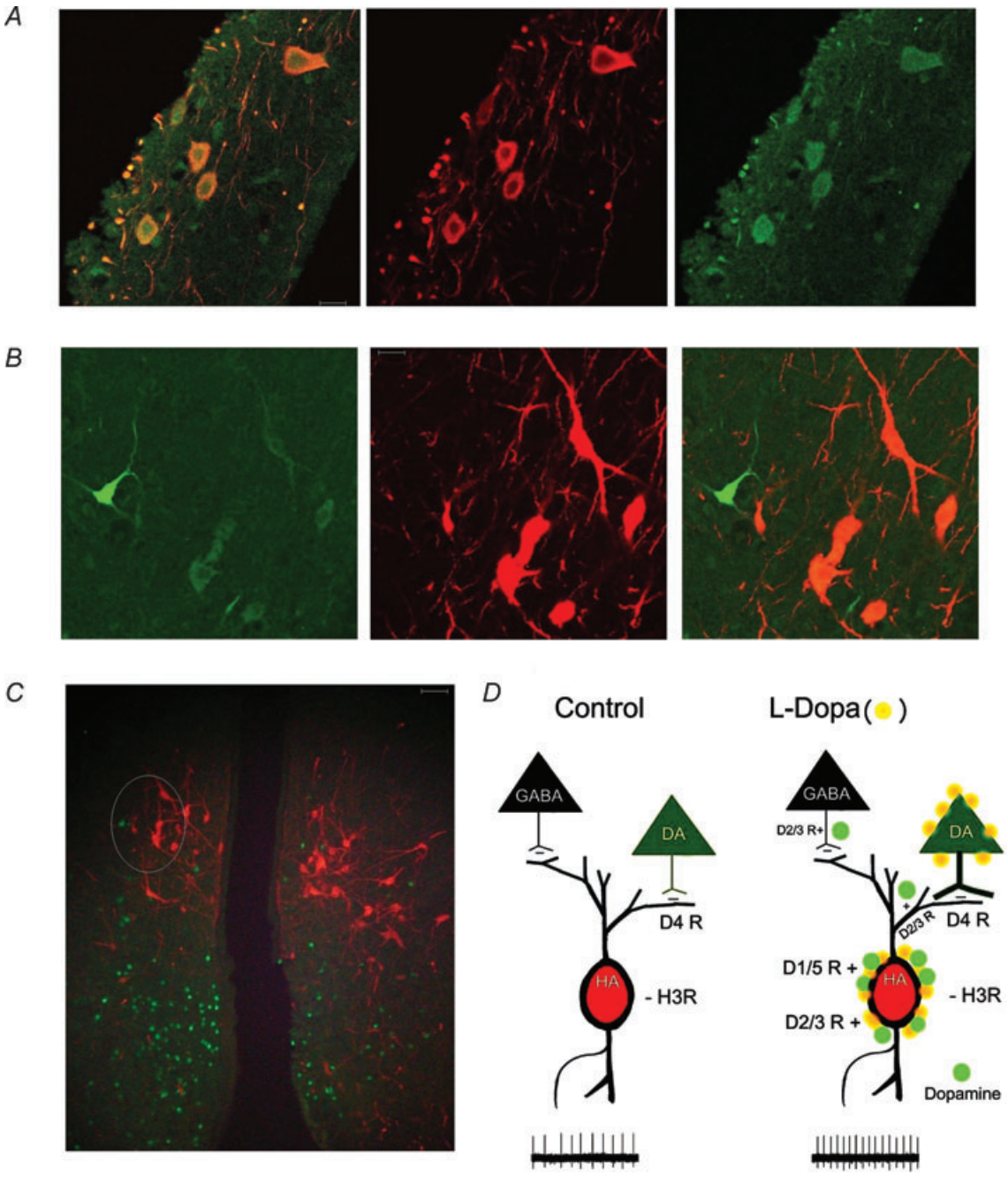

Figure 7. Dopamine–histamine interaction in the posterior hypothalamus
A, group of neurons in TMNv stained for histamine (revealed with cy3, red) and dopamine (revealed with AF488, green). *B*, dorsal TMN bordering dopaminergic neurons of posterior periventricular nucleus of the hypothalamus (slice in Fig. 2*Da*). This is an enlarged image from elliptic field indicated in *C*. Scale bars: *A* and *B*, 20 μm; *C*, 65 μm. Schematic drawing of dopaminergic and GABAergic inhibitory (–) inputs to the TMN neuron, which are overwhelmed by excitation under L-Dopa. Juxtacellular unit recordings are given for control and L-Dopa supplemented medium.

cellular markers in HDC KO and WT mice shows no difference between the two genotypes. *D*, in rat but not in mouse slices, the dopamine reuptake inhibitor nomifensine (1 μM) causes suppression of TMN firing, which is prevented by the D4 receptor antagonist L-745,870 (1 μM).

in the striatum of 6-OHDA lesioned rats and H3R blockade markedly improves motor coordination, indicating that histamine augments motor dyskinesia in PD and presumably counteracts L-Dopa therapy through H3R (Nowak *et al.* 2008).

Our study shows that L-Dopa changes the balance from the normally prevailing inhibitory dopaminergic tone on TMN neurons (D4R) to a dominant dopaergic excitation. The sensitivity of TMN neurons to L-Dopa ($EC_{50} = 15\ \mu M$) was surprisingly higher than the previously described sensitivity of substantia nigra dopaminergic neurons (Sebastianelli *et al.* 2008), whereas the potency of quinpirole in TMN neurons was strikingly low, when compared to the substantia nigra or VTA (Korotkova *et al.* 2002, 2007), where 10 μM are sufficient to block completely and irreversibly the firing of dopaminergic neurons. This is likely to be due to the low accessibility of dopamine receptors on TMN neurons for the bath applied substances and their much higher density/activation rate at the endogeneous dopamine release sites. Another explanation for the low sensitivity D1-like and D2-like receptors on TMN neurons could be their ubiquitous heteromerisation with H3Rs, which should lead to the reduction of receptor potency in the presence of histamine (Ferrada *et al.* 2008).

Our sleep–wake study in $HDC^{-/-}$ and WT mice demonstrates that wake promoting effects of quinpirole ($1\ mg\ kg^{-1}$) revert to sleep promoting in KO mice. In accordance with this, cocaine causes a smaller behavioural stimulation in $HDC^{-/-}$ mice than in WT (Brabant *et al.* 2007). On the other hand, modafinil-induced behavioural arousal seems to be independent of the histaminergic system as it is intact in histamine deficient mice (Parmentier *et al.* 2007). Despite activation of D2-like receptors in midbrain dopaminergic neurons (Korotkova *et al.* 2007), a clinically relevant dose of modafinil is not sufficient to increase the firing of rat TMN neurons through the low affinity D2-like receptors (our unpublished observation). In accordance with the proposed important role of the histaminergic system in the control of vigilance in PD patients, modafinil has only a small effect as an alertness enhancer in PD (Arnulf & Leu-Semenescu, 2009).

In conclusion we describe here a brain region displaying an action of L-Dopa superior to dopaminergic ligands (as seen in PD patients). In contrast to other arousal centres of the brain, the histaminergic system remains intact in PD and has become an attractive drug target for increasing alertness and improving motor control in PD patients. The normally existing inhibitory tone on TMN neurons through histaminergic H3 receptors and dopaminergic D4 receptors is overwhelmed under L-Dopa therapy, which stimulates histamine and dopamine release.

References

Anaclet C, Parmentier R, Ouk K, Guidon G, Buda C, Sastre JP, Akaoka H, Sergeeva OA, Yanagisawa M, Ohtsu H, Franco P, Haas HL & Lin JS (2009). Orexin/hypocretin and histamine: distinct roles in the control of wakefulness demonstrated using knock-out mouse models. *J Neurosci* **29**, 14423–14438.

Anichtchik OV, Rinne JO, Kalimo H & Panula P (2000). An altered histaminergic innervation of the substantia nigra in Parkinson's disease. *Exp Neurol* **163**, 20–30.

Arbuthnott G & Wright AK (1982). Some non-fluorescent connections of the nigro-neostriatal dopamine neurones. *Brain Res Bull* **9**, 367–368.

Arnulf I (2009). Results of clinical trials of tiprolisant in narcolepsy and Parkinson's disease. *Eur Neuropsychopharmacology* **19**, S204.

Arnulf I & Leu-Semenescu S (2009). Sleepiness in Parkinson's disease. *Parkinsonism Relat Disord* **15**(Suppl 3), S101–S104.

Brabant C, Quertemont E, Anaclet C, Lin JS, Ohtsu H & Tirelli E (2007). The psychostimulant and rewarding effects of cocaine in histidine decarboxylase knockout mice do not support the hypothesis of an inhibitory function of histamine on reward. *Psychopharmacology (Berl)* **190**, 251–263.

Cenni G, Blandina P, Mackie K, Nosi D, Formigli L, Giannoni P, Ballini C, Della CL, Mannaioni PF & Passani MB (2006). Differential effect of cannabinoid agonists and endocannabinoids on histamine release from distinct regions of the rat brain. *Eur J Neurosci* **24**, 1633–1644.

Drummond GB (2009). Reporting ethical matters in *The Journal of Physiology*: standards and advice. *J Physiol* **587**, 713–719.

Dziedzicka-Wasylewska M (2004). Brain dopamine receptors: research perspectives and potential sites of regulation. *Pol J Pharmacol* **56**, 659–671.

Dzirasa K, Ribeiro S, Costa R, Santos LM, Lin SC, Grosmark A, Sotnikova TD, Gainetdinov RR, Caron MG & Nicolelis MA (2006). Dopaminergic control of sleep-wake states. *J Neurosci* **26**, 10577–10589.

Ericson H, Watanabe T & Kohler C (1987). Morphological analysis of the tuberomammillary nucleus in the rat brain: delineation of subgroups with antibody against L-histidine decarboxylase as a marker. *J Comp Neurol* **263**, 1–24.

Eriksson KS, Stevens DR & Haas HL (2001*a*). Serotonin excites tuberomammillary neurons by activation of Na^+/Ca^{2+}-exchange. *Neuropharmacology* **40**, 345–351.

Eriksson KS, Sergeeva O, Brown RE & Haas HL (2001*b*). Orexin/hypocretin excites the histaminergic neurons of the tuberomammillary nucleus. *J Neurosci* **21**, 9273–9279.

Eriksson KS, Zhang S, Lin L, Lariviere RC, Julien JP & Mignot E (2008). The type III neurofilament peripherin is expressed in the tuberomammillary neurons of the mouse. *BMC Neurosci* **9**, 26.

Ferrada C, Ferre S, Casado V, Cortes A, Justinova Z, Barnes C, Canela EI, Goldberg SR, Leurs R, Lluis C & Franco R (2008). Interactions between histamine H3 and dopamine D2 receptors and the implications for striatal function. *Neuropharmacology* **55**, 190–197.

Ferrada C, Moreno E, Casado V, Bongers G, Cortes A, Mallol J, Canela EI, Leurs R, Ferre S, Lluis C & Franco R (2009). Marked changes in signal transduction upon heteromerization of dopamine D1 and histamine H3 receptors. *Br J Pharmacol* **157**, 64–75.

Fronczek R, Overeem S, Lee SY, Hegeman IM, van Pelt J, van Duinen SG, Lammers GJ & Swaab DF (2007). Hypocretin (orexin) loss in Parkinson's disease. *Brain* **130**, 1577–1585.

Haas HL & Reiner PB (1988). Membrane properties of histaminergic tuberomammillary neurones of the rat hypothalamus in vitro. *J Physiol* **399**, 633–646.

Haas HL, Sergeeva OA & Selbach O (2008). Histamine in the nervous system. *Physiol Rev* **88**, 1183–1241.

Haj-Dahmane S (2001). D2-like dopamine receptor activation excites rat dorsal raphe 5-HT neurons in vitro. *Eur J Neurosci* **14**, 125–134.

Inagaki N, Yamatodani A, Ando-Yamamoto M, Tohyama M, Watanabe T & Wada H (1988). Organization of histaminergic fibers in the rat brain. *J Comp Neurol* **273**, 283–300.

Jones BE (2005). From waking to sleeping: neuronal and chemical substrates. *Trends Pharmacol Sci* **26**, 578–586.

Khan ZU, Koulen P, Rubinstein M, Grandy DK & Goldman-Rakic PS (2001). An astroglia-linked dopamine D2-receptor action in prefrontal cortex. *Proc Natl Acad Sci U S A* **98**, 1964–1969.

Khan ZU, Mrzljak L, Gutierrez A, de la CA & Goldman-Rakic PS (1998). Prominence of the dopamine D2 short isoform in dopaminergic pathways. *Proc Natl Acad Sci U S A* **95**, 7731–7736.

Korotkova TM, Haas HL & Brown RE (2002). Histamine excites GABAergic cells in the rat substantia nigra and ventral tegmental area in vitro. *Neurosci Lett* **320**, 133–136.

Korotkova TM, Klyuch BP, Ponomarenko AA, Lin JS, Haas HL & Sergeeva OA (2007). Modafinil inhibits rat midbrain dopaminergic neurons through D2-like receptors. *Neuropharmacology* **52**, 626–633.

Li A, Guo H, Luo X, Sheng J, Yang S, Yin Y, Zhou J & Zhou J (2006). Apomorphine-induced activation of dopamine receptors modulates FGF-2 expression in astrocytic cultures and promotes survival of dopaminergic neurons. *FASEB J* **20**, 1263–1265.

Lin JS, Sergeeva OA & Haas HL (2011). Histamine H3-receptors and sleep-wake regulation. *J Pharmacol Exp Ther* **336**, 17–23.

Liu CQ, Hu DN, Liu FX, Chen Z & Luo JH (2008). Apomorphine-induced turning behavior in 6-hydroxydopamine lesioned rats is increased by histidine and decreased by histidine decarboxylase, histamine H1 and H2 receptor antagonists, and an H3 receptor agonist. *Pharmacol Biochem Behav* **90**, 325–330.

Loucif AJ, Woodhall GL, Sehirli US & Stanford IM (2008). Depolarisation and suppression of burst firing activity in the mouse subthalamic nucleus by dopamine D1/D5 receptor activation of a cyclic-nucleotide gated non-specific cation conductance. *Neuropharmacology* **55**, 94–105.

Mansour A, Meador-Woodruff JH, Bunzow JR, Civelli O, Akil H & Watson SJ (1990). Localization of dopamine D2 receptor mRNA and D1 and D2 receptor binding in the rat brain and pituitary: an in situ hybridization-receptor autoradiographic analysis. *J Neurosci* **10**, 2587–2600.

Memo M, Missale C, Carruba MO & Spano PF (1986). Pharmacology and biochemistry of dopamine receptors in the central nervous system and peripheral tissue. *J Neural Transm Suppl* **22**, 19–32.

Mercuri NB & Bernardi G (2005). The 'magic' of L-dopa: why is it the gold standard Parkinson's disease therapy? *Trends Pharmacol Sci* **26**, 341–344.

Mercuri NB, Calabresi P & Bernardi G (1990). Responses of rat substantia nigra compacta neurones to L-DOPA. *Br J Pharmacol* **100**, 257–260.

Monti JM & Monti D (2007). The involvement of dopamine in the modulation of sleep and waking. *Sleep Med Rev* **11**, 113–133.

Morgan S, Baker D & Huston JP (1998). Relationship between behavioral recovery from unilateral 6-OHDA lesion of the substania nigra and changes in the tuberomammillary-striatal projection as measured by HRP-labelling. *Restor Neurol Neurosci* **12**, 213–221.

Munsch T, Yanagawa Y, Obata K & Pape HC (2005). Dopaminergic control of local interneuron activity in the thalamus. *Eur J Neurosci* **21**, 290–294.

Nowak P, Bortel A, Dabrowska J, Biedka I, Slomian G, Roczniak W, Kostrzewa RM & Brus R (2008). Histamine H_3 receptor ligands modulate L-dopa-evoked behavioral responses and L-dopa derived extracellular dopamine in dopamine-denervated rat striatum. *Neurotox Res* **13**, 231–240.

Onali P, Olianas MC & Gessa GL (1985). Characterization of dopamine receptors mediating inhibition of adenylate cyclase activity in rat striatum. *Mol Pharmacol* **28**, 138–145.

Parmentier R, Anaclet C, Guhennec C, Brousseau E, Bricout D, Giboulot T, Bozyczko-Coyne D, Spiegel K, Ohtsu H, Williams M & Lin JS (2007). The brain H3-receptor as a novel therapeutic target for vigilance and sleep-wake disorders. *Biochem Pharmacol* **73**, 1157–1171.

Parmentier R, Kolbaev S, Klyuch BP, Vandael D, Lin JS, Selbach O, Haas HL & Sergeeva OA (2009). Excitation of histaminergic tuberomamillary neurons by thyrotropin-releasing hormone. *J Neurosci* **29**, 4471–4483.

Parmentier R, Ohtsu H, Djebbara-Hannas Z, Valatx JL, Watanabe T & Lin JS (2002). Anatomical, physiological, and pharmacological characteristics of histidine decarboxylase knock-out mice: evidence for the role of brain histamine in behavioral and sleep-wake control. *J Neurosci* **22**, 7695–7711.

Purba JS, Hofman MA & Swaab DF (1994). Decreased number of oxytocin-immunoreactive neurons in the paraventricular nucleus of the hypothalamus in Parkinson's disease. *Neurology* **44**, 84–89.

Ramanathan S, Tkatch T, Atherton JF, Wilson CJ & Bevan MD (2008). D2-like dopamine receptors modulate SKCa channel function in subthalamic nucleus neurons through inhibition of Cav2.2 channels. *J Neurophysiol* **99**, 442–459.

Sanchez-Lemus E & Arias-Montano JA (2004). Histamine H3 receptor activation inhibits dopamine D1 receptor-induced cAMP accumulation in rat striatal slices. *Neurosci Lett* **364**, 179–184.

Saper CB (2006). Staying awake for dinner: hypothalamic integration of sleep, feeding, and circadian rhythms. *Prog Brain Res* **153**, 243–252.

Saper CB, Sorrentino DM, German DC & de Lacalle S (1991). Medullary catecholaminergic neurons in the normal human brain and in Parkinson's disease. *Ann Neurol* **29**, 577–584.

Sebastianelli L, Ledonne A, Marrone MC, Bernardi G & Mercuri NB (2008). The L-amino acid carrier inhibitor 2-aminobicyclo[2.2.1]heptane-2-carboxylic acid (BCH) reduces L-dopa-elicited responses in dopaminergic neurons of the substantia nigra pars compacta. *Exp Neurol* **212**, 230–233.

Sergeeva OA, Chepkova AN, Doreulee N, Eriksson KS, Poelchen W, Monnighoff I, Heller-Stilb B, Warskulat U, Haussinger D & Haas HL (2003). Taurine-induced long-lasting enhancement of synaptic transmission in mice: role of transporters. *J Physiol* **550**, 911–919.

Sergeeva OA, Eriksson KS, Sharonova IN, Vorobjev VS & Haas HL (2002). $GABA_A$ receptor heterogeneity in histaminergic neurons. *Eur J Neurosci* **16**, 1472–1482.

Sergeeva OA, Kletke O, Kragler A, Poppek A, Fleischer W, Schubring SR, Gorg B, Haas HL, Zhu XR, Lubbert H, Gisselmann G & Hatt H (2010). Fragrant dioxane derivatives identify β1-subunit-containing $GABA_A$ receptors. *J Biol Chem* **285**, 23985–23993.

Sergeeva OA, Klyuch BP, Fleischer W, Eriksson KS, Korotkova TM, Siebler M & Haas HL (2006). P2Y receptor-mediated excitation in the posterior hypothalamus. *Eur J Neurosci* **24**, 1413–1426.

Sotnikova TD, Caron MG & Gainetdinov RR (2006). DDD mice, a novel acute mouse model of Parkinson's disease. *Neurology* **67**, S12–S17.

Stoof JC & Kebabian JW (1984). Two dopamine receptors: biochemistry, physiology and pharmacology. *Life Sci* **35**, 2281–2296.

Swanson LW (1982). The projections of the ventral tegmental area and adjacent regions: a combined fluorescent retrograde tracer and immunofluorescence study in the rat. *Brain Res Bull* **9**, 321–353.

Swanson LW (1992). *Brain Maps: Structure of the Rat Brain.* Elsevier, Amsterdam: The Netherlands.

Timmerman W, Deinum ME, Westerink BH & Schuiling GA (1995). Lack of evidence for dopamine autoreceptors in the mediobasal hypothalamus: a microdialysis study in awake rats. *Neurosci Lett* **195**, 113–116.

Vanhala A, Yamatodani A & Panula P (1994). Distribution of histamine-, 5-hydroxytryptamine-, and tyrosine hydroxylase-immunoreactive neurons and nerve fibers in developing rat brain. *J Comp Neurol* **347**, 101–114.

Von Economo C (1926). Die Pathologie des Schlafes. In *Handbuch der Normalen und Pathologischen Physiologie*, ed. von Bethe A, Bergmann GV, Embden G, *et al*. Springer, Berlin, vol. 17, pp. 591–610.

Weihe E, Depboylu C, Schutz B, Schafer MK & Eiden LE (2006). Three types of tyrosine hydroxylase-positive CNS neurons distinguished by dopa decarboxylase and VMAT2 co-expression. *Cell Mol Neurobiol* **26**, 659–678.

Yang CR, Bourque CW & Renaud LP (1991). Dopamine D2 receptor activation depolarizes rat supraoptic neurones in hypothalamic explants. *J Physiol* **443**, 405–419.

Zhu ZT, Shen KZ & Johnson SW (2002). Pharmacological identification of inward current evoked by dopamine in rat subthalamic neurons in vitro. *Neuropharmacology* **42**, 772–781.

Zoli M, Agnati LF, Tinner B, Steinbusch HW & Fuxe K (1993). Distribution of dopamine-immunoreactive neurons and their relationships to transmitter and hypothalamic hormone-immunoreactive neuronal systems in the rat mediobasal hypothalamus. A morphometric and microdensitometric analysis. *J Chem Neuroanat* **6**, 293–310.

Author contributions

O.A.S. designed the study, performed, analysed, interpreted *in vitro* experiments and drafted the manuscript. O.A.S. with the participation of S.L. performed immunohistochemistry and molecular biology. Y.Y., B.K. and S.L. performed, analysed and interpreted *in vitro* electrophysiological experiments at Heinrich-Heine-University Düsseldorf. J.-S.L. designed and performed sleep-wake-recordings assisted by S.L. and Q.Y. at INSERM-U628 in Lyon. P.B. and M.B.P. designed, performed and interpreted microdialysis experiments at the University of Florence. H.L.H. advised on experiments and drafting the article. All authors read and commented on the manuscript.

Acknowledgements

This work was supported by the DFG SE 1767, SFB 575/3 and 8, INSERM U628. We wish to thank Dr Hiroshi Ohtsu for the generous donation of HDC-knockout mice. The authors have no conflict of interest to disclose.